NON PROPORTIONAL LOADING EFFECTS ON FATIGUE CRACK INITIATION AND CRACK GROWTH PATH

L. Reis[1], M. Freitas[2] and B. Li[3]

[1] Dept. Engenharia Mecânica, Instituto Superior Técnico, Technical University of Lisbon
Av. Rovisco Pais, 1049-001 Lisboa, Portugal
E-mail: lreis@ist.utl.pt
Tfno: 351 218417481 Fax: 351 218147915

[2] Dept. Engenharia Mecânica, Instituto Superior Técnico, Technical University of Lisbon
Av. Rovisco Pais, 1049-001 Lisboa, Portugal
E-mail: mfreitas@dem.ist.utl.pt
Tfno: 351 218417459 Fax: 351 218147915

[3]Dept. Engenharia Mecânica, Instituto Superior Técnico, Technical University of Lisbon
Av. Rovisco Pais, 1049-001 Lisboa, Portugal
E-mail: bli@ist.utl.pt
Tfno: 351 218417481 Fax: 351 218147915

RESUMEN

Os componentes e as estruturas na industria estão, na maioria das situações, submetidos a estados de tensão multiaxial. Existem vários modelos sobre fadiga multiaxial propostos na literatura. Uma eficiente análise em fadiga de componentes e estruturas submetidas a carregamento multiaxial requer a validação de modelos e abordagens apropriadas. Neste artigo são apresentados o trabalho experimental e teórico realizados sobre o comportamento mecânico do aço estrutural DIN42CrMo4, temperado e revenido, em fadiga multiaxial. Os ensaios foram realizados utilizando uma máquina servo-hidraulica biaxial. Foram consideradas diversas trajectórias de carregamento, compostas por tracção/torção cíclicas com diferentes rácios entre a componente normal e de corte. Posteriormente os resultados experimentais obtidos em fadiga são analisados e correlacionados por um parâmetro de fadiga, o qual avalia o dano por fadiga num novo espaço de tensão de corte. Foram ainda utilizados modelos de plano critico para correlacionar os resultados obtidos na medição da orientação dos planos de iniciação de fenda. Os resultados mostram uma forte influência dos parâmetros estudados das trajectórias de carregamento na vida a fadiga e na orientação dos planos de iniciação de fenda.

ABSTRACT

Components and structures in industry are generally subjected to multiaxial stress states. There are many multiaxial fatigue models proposed in the literature. For efficient computational fatigue analysis of components and structures, it is required to carry out further validations of multiaxial fatigue models and appropriate approaches for shear stress evaluation under service loading conditions. In this paper, multiaxial fatigue tests were carried out on a quenched and tempered low alloy steel (DIN 42CrMo4) for a wide range of loading paths of tension and torsion. A large number of tests are available for the analysis of the influence of the loading paths on crack initiation, crack path growth and life prediction. Critical plane approaches were used to correlate the results of the experimental tests with the prediction of the crack path orientation and life tests. Results show a strong influence of the studied parameters chosen for the loading paths on fatigue life and crack initiation and are discussed in this paper taking into account the evolution of the stress-strain due to the loading path.

PALABRAS CLAVE: Multiaxial fatigue models, Fatigue strength, Life prediction, Crack path, Crack initiation.

1. INTRODUCTION

Most engineering components are subjected to multiaxial states of stress and strain due to the presence of stress raisers such as notches or holes. Moreover, components such as crankshafts, propeller shafts, vehicle axles, shafts of flywheels, and structures such as submarine hulls and pressure vessels undergo multiaxial fatigue loading resulting in biaxial and triaxial stress states. Therefore, growing research efforts have been paid to study the cyclic deformation behavior and fatigue life prediction of engineering materials and components under multiaxial loading conditions. In addition to the study on the fatigue life, a recent trend is to study the crack growth orientation, since the prediction of potential crack path as well as fatigue lifetime is very important for safety evaluations and failure mode analyses.

In real engineering structures, there are many factors influencing the fatigue crack paths, such as the material type (microstructure), structural geometry and loading path, etc. It is widely believed that fatigue crack nucleation and early crack growth are caused by cyclic plasticity.

For efficient computational fatigue analysis of components and structures, it is required to carry out further validations of multiaxial fatigue models and appropriate approaches for shear stress evaluation under service loading conditions [1].

For structural steels, the shear stress amplitude is one of the important parameters in the formulations of multiaxial fatigue damage models. Conventionally, the shear stress amplitude was usually evaluated in the shear stress space based on the von Mises equivalence ($\tau=\sigma/\sqrt{3}$) or the maximum shear stress equivalence ($\tau=\sigma/2$) for the multiaxial loading conditions. However, the relationship of the equivalent shear stress related to the axial stress component may vary significantly depending on the type of the material. For example, the ratio of the torsion fatigue limit over the bending fatigue limit τ_{-1}/f_{-1} varies from 0.5 for mild metals to 1 for brittle metals [2].

This paper presents data from multiaxial fatigue tests that were carried out on a quenched and tempered low alloy steel for a wide range of loading paths of tension and torsion. For each loading path the following parameters were changed: in phase and out of phase loading, sinusoidal, triangular and square waves and non-proportionality between tension and torsion.

A large number of tests are therefore available for the analysis of the influence of the loading paths on crack initiation, crack path growth and life prediction. Critical plane approaches (either stress based or strain based approaches) were used to correlate the results of the experimental tests with the prediction of the crack path orientation and life tests.

Results show a strong influence of the studied parameters of the loading paths on fatigue life and crack initiation and are discussed in this paper taking into account the evolution of the stress-strain due to the loading path.

2. MATERIAL DATA, SPECIMEN FORM AND TEST PROCEDURE

The DIN42CrMo4 quenched and tempered high strength steel is the material used in this work. The chemical composition is shown in table 1. Monotonic and cyclic mechanical properties are shown in table 2 (cyclic properties obtained by fitting the test results). The geometry and dimensions of the specimen are shown in figure 1.

Table 1. Chemical composition of the material studied 42CrMo4 (in wt%)

C	Si	Mn	P	Cr	Ni	Mo	Cu
0.39	0.17	0.77	0.02	1.10	0.30	0.16	0.21

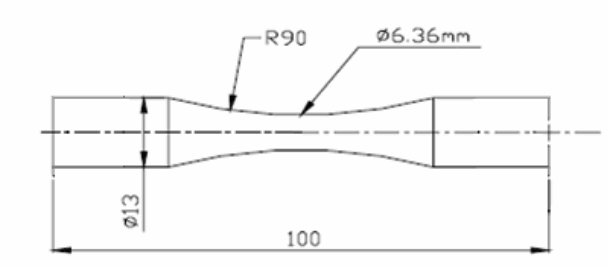

Figure 1. Specimen geometry for biaxial cyclic tension-compression with cyclic torsion tests

Table 2. Monotonic and cyclic mechanical properties of the studied material

Tensile strength	σ (MPa)	1100
Yield strength	$\sigma_{0.2,monotonic}$ (MPa)	980
Elongation	A (%)	16
Young's modulus	E (GPa)	206
Yield strength	$\sigma_{0.2,cyclic}$ (MPa)	540
Strength coefficient	K´(MPa)	1420
Strain hardening exponent	n´	0.12
Fatigue strength coefficient	σ_f´(MPa)	1154
Fatigue strength exponent	b	-0.061
Fatigue ductility coefficient	ε_f´	0.18
Fatigue ductility exponent	c	-0.53

Tests of biaxial cyclic tension-compression with cyclic torsion were performed by a biaxial servo-hydraulic machine, shown in figure 2. Test conditions were as follows: frequency 4-6 Hz at room temperature and laboratory air. Tests ended up when the specimens were completely broken.

To study the effects of the multiaxial loading paths and in particular both the effect of axial component and the effect of torsional component on the fatigue life, a series of loading paths were applied in the experiments as shown in tables 3 and 4. For each loading path the following parameters were changed: in phase and out of phase loading, sinusoidal, triangular and square waves and non-proportionality between tension and torsion.

Table 3. Reference multiaxial fatigue loading paths

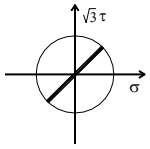 case I	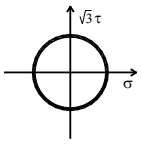 case II
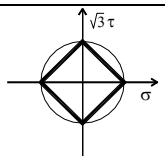 case III	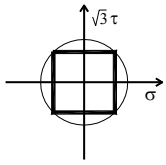 case IV

Table 4. Variations of the reference multiaxial fatigue loading paths

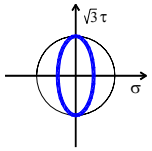 case II_A	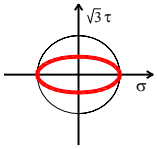 case II_B
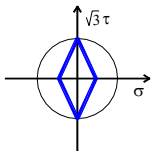 case III_A	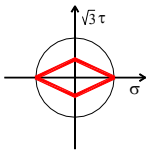 case III_B
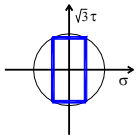 case IV_A	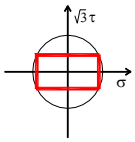 case IV_B

Figure 2. Biaxial testing machine (Instron 8874)

3. THEORETICAL ANALYSIS OF FATIGUE LIFE AND CRACK INITIATION

Many multiaxial fatigue models have been proposed in the last decades [1]. Among several parameters and constants, the shear stress amplitude is one of the most important parameters in the formulations of the multiaxial fatigue damage models, in high cycle fatigue regime. Considering the orientation of the potential crack initiation plane, critical plane models are used to analyze it.

3.1. Equivalent stress range of ASME code

The ASME Boiler and Pressure Vessel code Procedure [4] is based on the von Mises hypothesis, but employs the stress difference $\Delta\sigma_i$ between to two arbitrary instants t_1 and t_2:

$$\Delta\sigma_{eq} = \frac{1}{2\sqrt{2}}\left\{\left(\Delta\sigma_x - \Delta\sigma_y\right)^2 + \left(\Delta\sigma_y - \Delta\sigma_z\right)^2 + \left(\Delta\sigma_z - \Delta\sigma_x\right)^2 + 6\left(\Delta\tau_{xy}^{\ 2} + \Delta\tau_{yz}^{\ 2} + \Delta\tau_{xz}^{\ 2}\right)\right\}^{1/2} \quad (1)$$

where the equivalent stress range $\Delta\sigma_{eq}$ is maximized with respect to time.

Eq. (1) produces a lower equivalent stress range, for some conditions, in out-of-phase than the in-phase loading, leading an increase of the fatigue life, which is in contradiction with experimental results.

3.2. MCE approach for evaluating shear stress amplitude

Among many multiaxial models, the Sines [5] and the Crossland [6] are two important criteria, which are formulated by the amplitude of the second deviatoric stress invariant and the hydrostatic stress P_H:

$$\sqrt{J_{2,a}} + k(N)P_H = \lambda(N) \quad (2)$$

where *k(N)* and *λ(N)* denote material parameters for a given life *N*.

Crossland suggested using the maximum value of the hydrostatic stress $P_{H,max}$ instead of the mean value of hydrostatic stress $P_{H,m}$ used by Sines in the Eq.(2). A physical interpretation of the criterion expressed in Eq.(2) is that for a given cyclic life *N,* the permissible amplitude of the root-mean-square of the shear stress over all planes is a linear function of the normal stress averaged over all planes. Besides, from the viewpoint of computational efficiency, the stress-invariant based approach such as Eq. (2) is easy to use and computationally efficient.

In practical engineering design, the Sines and Crossland criteria have found successful applications for proportional multiaxial loading. For non-proportional multiaxial loading, it has been shown that the Sines and Crossland criteria can also yield better prediction results

by using improved method MCE for evaluating the effective shear stress amplitude of the non-proportional loading path.

The evaluation of shear stress amplitude is a key issue for fatigue estimations using Eq. (2). The definition of the square root of the second invariant of the stress deviator is:

$$\sqrt{J_2} \equiv \sqrt{\frac{1}{6}\left\{\left(\sigma_{xx}-\sigma_{yy}\right)^2+\left(\sigma_{yy}-\sigma_{zz}\right)^2+\left(\sigma_{zz}-\sigma_{xx}\right)^2\right\}} + \sqrt{\left\{\left(\sigma_{xy}\right)^2+\left(\sigma_{yz}\right)^2+\left(\sigma_{zx}\right)^2\right\}} \quad (3)$$

One direct way to calculate the amplitude of $\sqrt{J_2}$ is:

$$\sqrt{J_{2,a}} \equiv \sqrt{\frac{1}{6}\left\{\left(\sigma_{xx,a}-\sigma_{yy,a}\right)^2+\left(\sigma_{yy,a}-\sigma_{zz,a}\right)^2+\left(\sigma_{zz,a}-\sigma_{xx,a}\right)^2\right\}} + \sqrt{\left\{\left(\sigma_{xy,a}\right)^2+\left(\sigma_{yz,a}\right)^2+\left(\sigma_{zx,a}\right)^2\right\}} \quad (4)$$

Eq.(4) is applicable for proportional loading, where all the stress components vary proportionally. However, when the stress components vary non-proportionally (for example, with phase shift between the stress components), Eq.(4) gives the same result with that of proportional loading condition. In fact, the non-proportionality has influence on the shear stress amplitude generated by multiaxial loading. Therefore, a new methodology is needed.

The longest chord (LC) approach is one of the well-known approaches as summarized by Papadopoulos [2], which defines the shear stress amplitude as half of the longest chord of the loading path, denoted as D/2.

The MCC approach [2] defines the shear stress amplitude as the radius of the minimum circle circumscribing to the loading path. On the basis of MCC approach, a new approach, called the minimum circumscribed ellipse (MCE) approach [3], was proposed to compute the effective shear stress amplitude taking into account the non-proportional loading effect. The load traces are represented and analyzed in the transformed deviatoric stress space, where each point represents a value of $\sqrt{J_2}$ and the variations of $\sqrt{J_2}$ are shown during a loading cycle. The schematic representation of the MCE approach and the relation with the minimum circumscribed circle (MCC) approach are illustrated in figure 3:

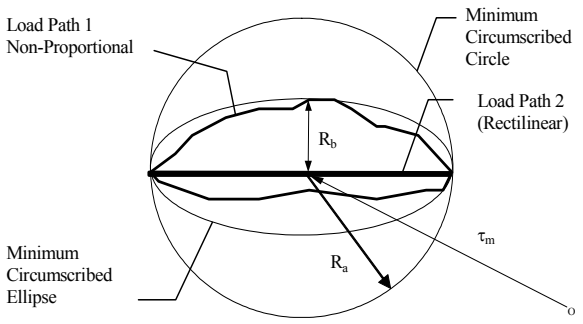

Figura 3. The MCC and MCE circumscribing to shear stress traces, Ra and Rb are the major and minor radius of MCE, respectively.

The idea of the MCE approach is to construct a minimum circumscribed ellipse that can enclose the whole loading path throughout a loading block in the transformed deviatoric stress space. Rather than defining $\sqrt{J_{2,a}} = R_a$ by the minimum circumscribed circle (MCC) approach, a new definition of was proposed [3], where Ra and Rb are the lengths of the major semi-axis and the minor semi-axis of the minimum circumscribed ellipse respectively.

The ratio of Rb/Ra represents the non-proportionality of the shear stress path. The important advantage of this new MCE approach is that it can take into account the non-proportional loading effects in an easy way.

As shown in figure 3, for the non-proportional loading path 1, the shear stress amplitude is defined as:

$$\sqrt{J_{2,a}} = \sqrt{R_a^2 + R_b^2} \quad (5)$$

For the proportional loading path 2, it is defined as $\sqrt{J_{2,a}} = R_a$ since R_b is equal to zero (rectilinear loading trace).

3.3. Critical plane approaches for evaluating crack plane orientation

For the biaxial loading cases shown in Tables 3 and 4, the potential crack plane orientation is analyzed by various critical plane models and energy-based critical plane models, such as the Findley, the Brown-Miller, the Fatemi-Socie, the Smith-Watson-Topper and the Liu´s criteria. Since the damage parameter formulations of some of the models (the Findley, the Brown-Miller and the Fatemi-Socie) require material dependent parameters, experiments were carried out firstly to determine the material dependent parameters for both materials, which are applied in the theoretical analyses of the crack plane orientations in this section. These models are well-known [1, 7] and due to space limitation of this paper are not presented here.

4. RESULTS AND DISCUSSIONS

4.1. Experimental cyclic stress-strain behavior under proportional and non-proportional loading with von Mises parameter

Proportional and non-proportional cyclic tests were conducted in the plane (σ, $\sqrt{3}\tau$). Non-proportional cyclic tests were conducted with the square, rectangle up and rectangle down, circle, ellipse down, ellipse up, losange, losange up and losange down loading paths, respectively (see tables 3 and 4). Figures 4 and 5 show the evolution of experimental life with equivalent von Mises stress parameter for cases I, II, II_A, II_B, III, III_A and III_B.

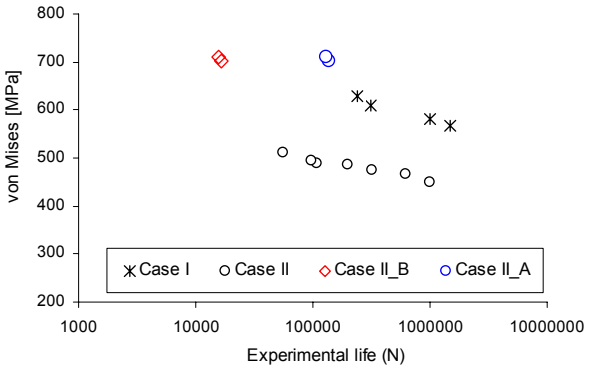

Figure 4. Evolution of experimental life with equivalent von Mises stress: cases I, II, II_A and II_B

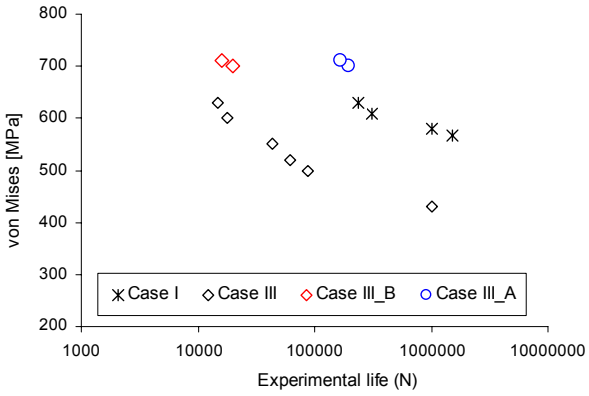

Figure 5. Evolution of experimental life with equivalent von Mises stress: cases I, III, III_A and III_B

From figures 4 and 5 it is shown that the von Mises parameter gives a big scatter when correlating the experimental results. In both pictures, it seems that there's two tendencies, one for proportional loading, case I, with cases II_A and III_A (strong torsional component) and another one with cases II, III, II_B and III_B (strong axial component). It can also be observed that cases II_A and III_A are the least severe together with the proportional case I. This means that a greater torsional component, as compared with the axial one, has not so strong influence in the fatigue life strength.

4.2. Experimental cyclic stress-strain behavior under proportional and non-proportional loading with new fatigue parameter

In order to get better correlations, the new shear stress space parameter with the equivalence $\tau=0.65*\sigma$ is used for the shear stress amplitude evaluations under multiaxial loading conditions. The parameter (Ta+Sig_h) is obtained from Eq. (2) with the shear stress amplitude calculated from Eq. (5).

Figure 6 present all the results obtained from the variations of the reference multiaxial fatigue loading paths. It can be observed that there's a good correlation between the data. The present work is part of continuous research in this matter and these results give some confidence in the upcoming work.

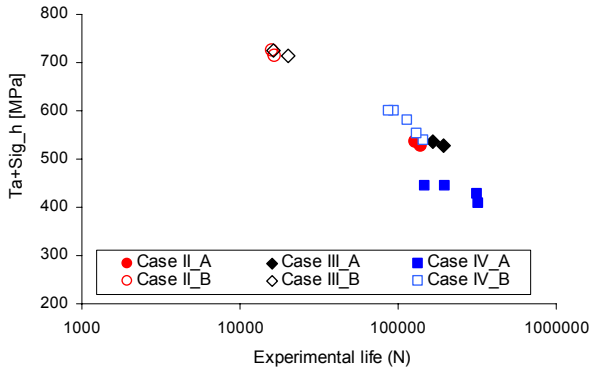

Figure 6. Evolution of the new fatigue parameter with experimental life: cases II_A, II_B, III_A, III_B, IV_A and IV_B

4.2. Fractographic analyses of the fatigue failure plane orientations

Fractographic analysis of the macroscopic plane of crack initiation and early crack growth were carried out, using an optical microscope at a magnification between 10 and 100 times. Some of the specimens were also analysed in the SEM microscope. The measurement of the crack initiation plane orientation was carried out as follows: firstly, the crack initiation was identified, as indicated by a white arrow on the left side in Figure 7; then, the specimen was analysed in a 3D measurement device and the angle between the crack initiation plane and the longitudinal axis was accurately measured, as shown on the right side of Figure 7. This procedure and one example for each loading path are shown in figure 7.

The measured values of the crack orientations are presented in Table 5. For the predictions of crack orientations and early growth investigated in this paper, the shear-based models (Brown-Miller, Findley, Wang-Brown, Fatemi-Socie and Liu II) must be analysed.

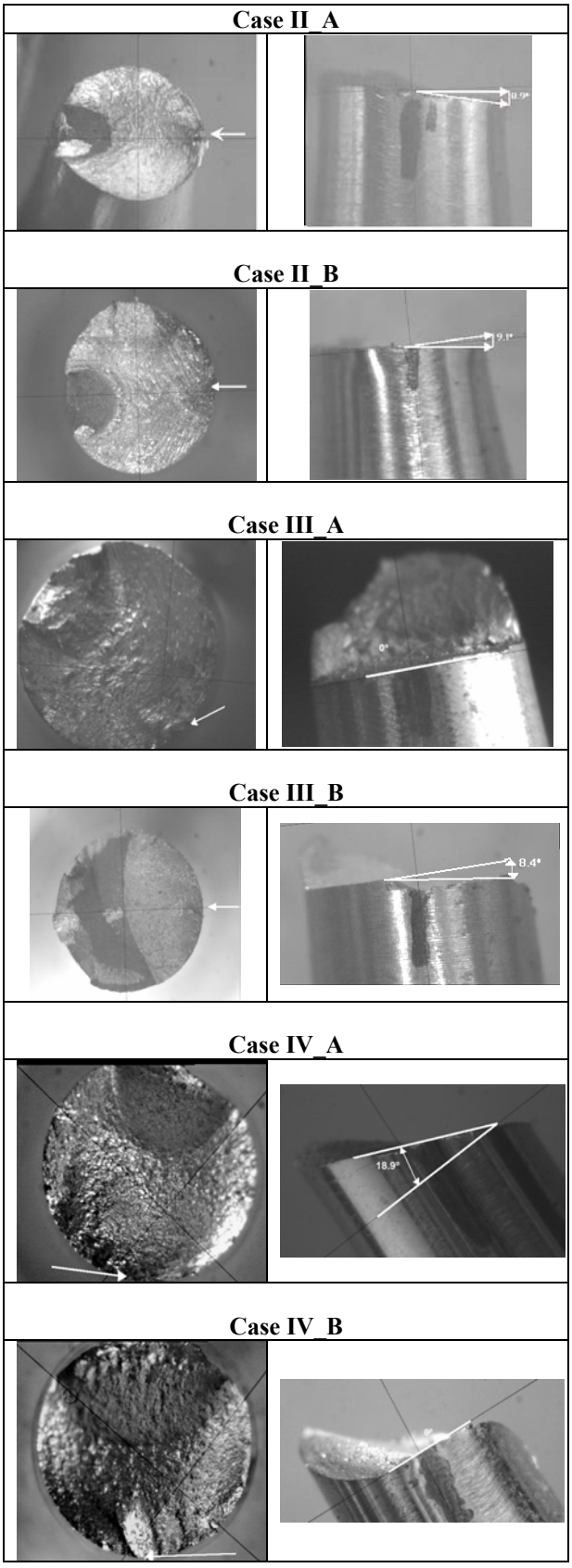

Figure 7. Fractographic analyses of the fatigue failure plane orientations for each type of loading path.

Table 5. Comparison of the measured crack plane with predictions by the critical planes

	Multiaxial Loading Paths					
	Case II_A	Case II_B	Case III_A	Case III_B	Case IV_A	Case IV_B
Measured	**7.8º**	**18.9º**	**3.85º**	**4.2º**	**15.2º**	**11.6º**

From the results shown it is observed that the non proportionality between tension and torsion components has a strong influence on crack plane orientation, despite they have an equivalent loading path. Further studies are being carried out on this subject.

5. CONCLUSIONS

Experimental results of multiaxial loading show that the ratio between normal stress component and shear stress component has a strong influence to fatigue damage and consequently in fatigue life.

The shear stress space used for the evaluation of the shear stress amplitude of multiaxial loading conditions should be appropriate for the material type.

The loading paths have a significant influence on the fatigue crack plane orientations.

ACKNOWLEDGEMENTS

Financial support of this work by FCT - Fundação para Ciência e Tecnología (Portuguese Foundation for Science and Technology) is gratefully acknowledged.

REFERENCES

[1] Socie D. F. and Marquis G. B. Multiaxial Fatigue, SAE, Warrendale, PA 15096-0001, 2000.
[2] Papadopoulos, I.V., Davoli, P., Gorla, C., Fillipini, M.and Bernasconi, A. A comparative study of multiaxial high-cycle fatigue criteria for metals. IJF, Vol. 19, Nº3, pp. 219-235.
[3] M. de Freitas, B. Li and J.L.T. Santos, Multiaxial Fatigue and Deformation: Testing and Prediction, ASTM STP 1387, S. Kaluri and P.J. Bonacuse, Eds., ASTM, West Consh, 2000, PA, pp.139-156.
[4] ASME Code Case N-47-23 (1988) Case of ASME Boiler and Pressure Vessel Code, ASME.
[5] Sines, G., (1959) Metal Fatigue, (edited by G. Sines and J.L.Waisman), McGraw Hill, N.Y, pp.145-169.
[6] Crossland, B., (1956) Proc. Int. Conf. on Fatigue of Metals, Inst. of Mech. Eng, London, pp.138-149.
[7] L. Reis, B. Li and M. de Freitas. Validation of multiaxial fatigue models for structural steels. Proced. of "XXII ENCUENTRO DEL GRUPO ESPAÑOL DE FRACTURA", Almagro, Espana, Vol. 22, pp. 347- 352, 9-11 de Março de 2005.